ARCHITECTURAL RESEARCH, Vol. 10, No. 1(June 2008), pp. 1-11

Fire Behavior of Steel Columns Encased by Damaged Spray-applied Fire Resistive Material

Yoon Keun Kwak, Stephen Pessiki and Kihyon Kwon
Department of Architectural Engineering, Kumoh National Institute of Technology, Gumi, Gyeong-Buk, Korea
Department of Civil & Environmental Engineering, Lehigh University, Bethlehem, PA, USA
Department of Civil & Environmental Engineering, Lehigh University, Bethlehem, PA, USA

Abstract

A Steel column with damaged spray-applied fire resistive material (SFRM) may exhibit reduced structural performance due to the effects of elevated temperature during fire events. Thus, the fire load behavior of steel columns with removed or reduced SFRM needs to be examined to predict the structural damage by fire. FEM analyses were performed for the flange thinning removal models in which the SFRM was reduced as a constant strip in thickness at the top flange of the column. The temperature results for all models obtained from the heat transfer analyses were included as an initial condition in the FEM structural analyses.
In this study, the results of analysis show that even small remnants of SFRM led to an effective reduction of temperature at any given fire duration, and improved significantly the axial load capacity of a column as compared to the complete removal cases of SFRM.

Keywords : SFRM, Fire Load, Fire Duration, Heat Transfer Analysis, Flange Thinning Removal Model

1. INTRODUCTION

1.1 Objective

Current practice in steel building construction is to use fire protection materials such as spray-applied fire resistive material (SFRM) to thermally protect structural steel columns in fire. The thickness of SFRM is usually based on fire duration, column weight, and column cross-section perimeter. During construction or occupancy, the SFRM may become damaged. Damage may be complete removal or reduced in thickness of SFRM. A steel column with damaged SFRM may exhibit reduced structural performance due to the effects of elevated temperature during fire events. Thus, the fire load behavior of steel columns with removed or reduced SFRM needs to be examined to predict the structural damage by fire.

The objective of this research is to investigate the temperature distributions and the axial load behavior of steel columns protected by damaged SFRM during the action of fire.
Analysis is performed to examine the fire load behavior of steel columns with damaged SFRM subjected to concentric axial compression. Nonlinear heat transfer analyses are performed to predict the temperature distribution in the steel columns under the action of the ASTM E-119 curve. Nonlinear structural analyses are then performed to elevate the influence of temperature on column axial load behavior. In current research, ABAQUS was selected to carry out heat transfer and structural analysis of steel columns.

1.2 Background

A considerable amount of research has been carried out for steel columns in fire. Lie and Stanzak (1973) investigated the fire resistance of steel columns protected by relatively low-density materials, and explained the mechanism of heat transfer from a fire through insulation to the steel core. During fire action, the temperature distribution of thermally protected steel column was investigated by Hyeon et al. (1990). It was suggested that the required minimum thickness of insulation can be affected by various construction conditions. Tomecek and Mike (1993) and Ryder et al. (2002) studied the effect of partial loss of fire-protection material on the fire resistance of steel columns. A two-dimensional finite element heat transfer analysis was used to compare the thermal response of steel columns with lost protection material when exposed to fire. Nonlinear heat transfer analyses were performed, and nonlinear structural analyses were not included in the study. Poh and Bennetts (1995) studied unprotected steel column behavior at elevated temperatures. Steel columns were analyzed using a moment-curvature approach, and nonlinear behavior of load-bearing steel columns was investigated. Franssen et al. (1998) and Talamona et al. (1997) studied stability issues of steel columns in fire. In their studies, the behavior of steel columns subjected to axial compressive forces was investigated both numerically and experimentally. Concentrically loaded as well as eccentrically loaded columns were considered. According to the experimental study performed by Kwon et al. (2002), the allowable temperature of 538 °C, which can conservatively preserve structural safety of column and beam exposed to fire, was introduced. Huang and Tan

(2003) studied analytical fire resistance of axially restrained steel columns. A linear spring was modeled at the column top in order to consider the axial restraint of upper-story structure on the isolated heated column. Koo et al. (2004) investigated the effect of elevated temperature for the lateral-torsional buckling of H-beams. The analytical study on the fire-resisting capacity of the iTECH beam was conducted to investigate load ratio and moment redistribution according to temperature elevation (Min et al., 2005).

Most of the studies on steel columns protected partially by damaged fire protection materials during fire events have been limited to investigation on thermal responses. However, it is also important to observe the structural degradation of a steel column as well as its thermal responses when exposed to fire. Thus, it is necessary that fire load behavior of steel columns encased by damaged SFRM is investigated during the action of fire.

Lee, Pessiki and Kohno (2006) carried out heat transfer and structural analyses of a series of steel box column fire tests performed by Kohno and Masuda (2003), and verified the effectiveness of analytical approaches for fire events. The same technique was also used in the study performed by Kwon et al. (2006). The validated approaches are herein employed.

2. MATERIAL PROPERTIES OF STEEL AND SFRM

2.1 Properties of Steel

A992 Grade 50(345Mpa) hot-rolled type mild steel is considered in the current study. The standard value for the density of structural steel is 7850kg/m^3. The thermal properties of steel are thermal conductivity, specific heat, emissivity, and coefficient of thermal expansion.

The thermal conductivity versus temperature relationship suggested by the Eurocode 3 is given in Equation (1) and (2), and it is shown graphically in Figure1.

$$K=54-(Ts/30) \quad \text{for } 20°C < Ts < 800°C \qquad (1)$$

$$K=27.3 \quad \text{for } Ts>800°C \qquad (2)$$

where k is the conductivity in W/m°C, and Ts is the steel temperature in °C.

As shown in Figure 1, the thermal conductivity tends to decrease with an increase in temperature, and stays constant above 800°C. Figure 1 also includes the thermal conductivity versus temperature relationship given in ASCE SFP. The two curves do not differ significantly.

The specific heat versus temperature relationship suggested by the Eurocode 3 is given in Equation (3) through (6), and it is shown graphically in Figure 2.

$$C=425+0.773Ts-0.00169Ts^2+2.22\times10^{-6}Ts^3$$

$$\text{for } 20°C<Ts<600°C \qquad (3)$$

$$C=666-13002/(Ts-738)$$

$$\text{for } 600°C<Ts<735°C \qquad (4)$$

$$C=545-17820/(Ts-731)$$

$$\text{for } 735°C<Ts<900°C \qquad (5)$$

$$C=650$$

$$\text{for } Ts>900°C \qquad (6)$$

where C is the specific heat in J/kg°C, and Ts is the steel temperature in °C.

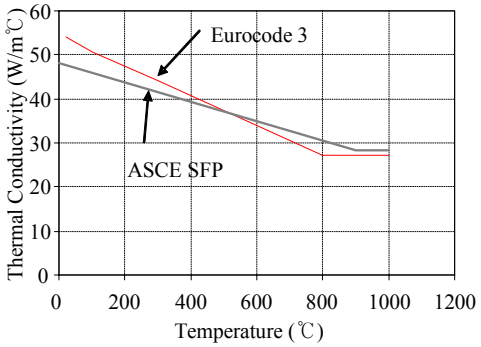

Figure 1. Conductivity versus temperature for conventional steel in the Eurocode 3 and ASCE SFP.

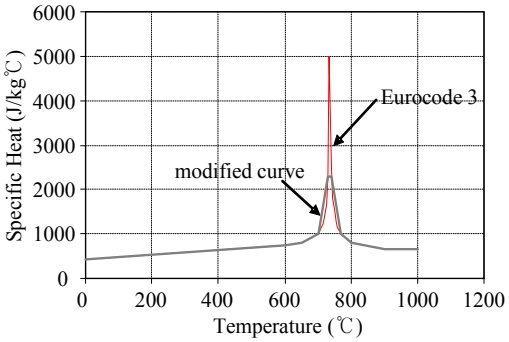

Figure 2. Specific heat versus temperature for conventional steel in the Eurocode 3 and modified specific heat.

As shown in Figure 2, the specific heat tends to increase with an increase in temperature up to 700°C, peaks near 735°C, and then tends to decrease after 735°C. The specific heat relationship given in the Eurocode 3 was modified in this research. Figure 2 compares the original Eurocode 3 specific heat with a modified specific heat relationship. This modification was necessary to run the finite element model in a stable manner. The sharp peak in the Eurocode 3 relationship leads to numerical difficulty in solution convergence. The modification provides the same area under each curve.

The radiation is the major heat transfer mechanism by which heat is transmitted in to the steel column by the fire. Thus, an appropriate value of steel surface emissivity is required to evaluate the steel temperatures correctly. However, because the emissivity depends on surface

conditions, it is not simple to determine the emissivity for a given member unless the emissivity is determined through a test. Table 1 shows steel emissivity values from the literature. A constant emissivity of 0.8 was used for the steel surface emissivity in this study.

The stress-strain relationship of steel at elevated temperatures is the most important parameter to predict structural performance of the member exposed to fire.

Table 1. Steel emissivity values from the literature.

Reference	Emissivity
Eurocode 3 (2001)	0.625
Wang (2002)	0.7
ASCE SFP (1992)	0.9
Holman (1981)	0.8 (oxidized)
Lamont et al. (2001)	0.7
Bejan (1993)	0.79
Siegel et al. (1980)	0.3 (polished) 0.81 (oxidized)
Quinne et al. (1992)	0.3 (polished) 0.8 (oxidized)

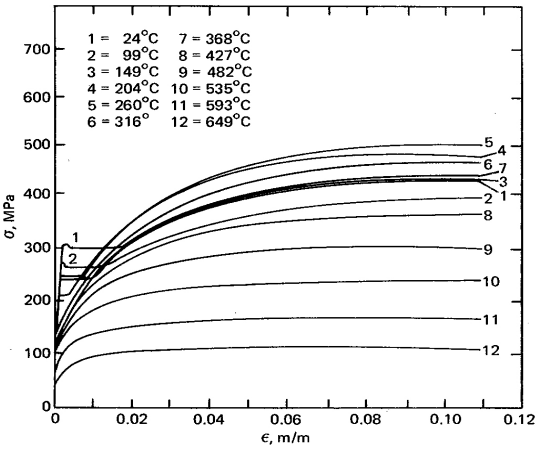

Figure 3. Stress-strain relationship for ASTM A36 steel at elevated temperatures (SFPE Handbook of Fire Protection Engineering, 1988).

Figure 3 shows the experimentally obtained stress-strain relationship of ASTM A36 steel at elevated temperatures as test results (SFPE Handbook of FPE, 1988). As shown in the Figure 3, the steel material degrades as temperature increases, and the shape of the stress-strain curves changes depending on temperatures. Figure 4 shows stress-strain relationships of the A992, Grade 50 steel (Fy=345Mpa) used in the steel column fire analysis at various temperatures, computed from the Eurocode 3 material model. Based on the stress-strain relationship shown in Figure 4, the elastic modulus of the A992, Grade 50 steel is plotted in Figure 5, and proportional limits and effective yield strength are shown in Figure 6 for various temperatures.

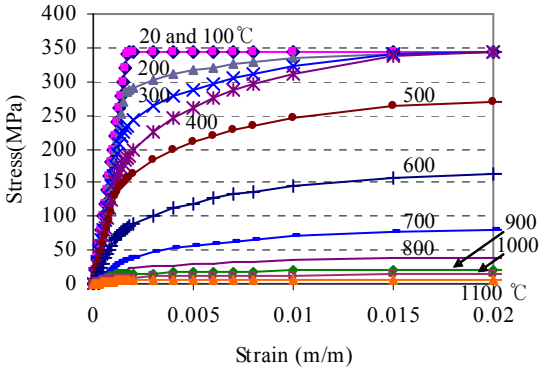

Figure 4. Stress-strain relationship of the A992, Grade 50 steel generated using the Eurocode 3.

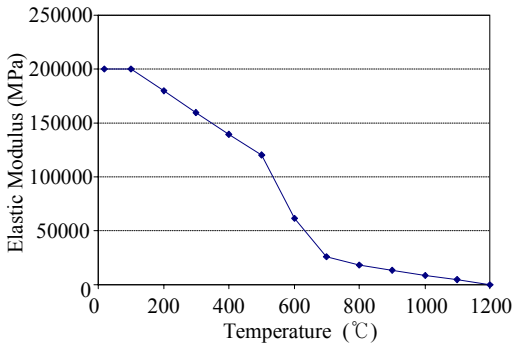

Figure 5. Elastic modulus versus temperature for the A992, Grade 50 steel.

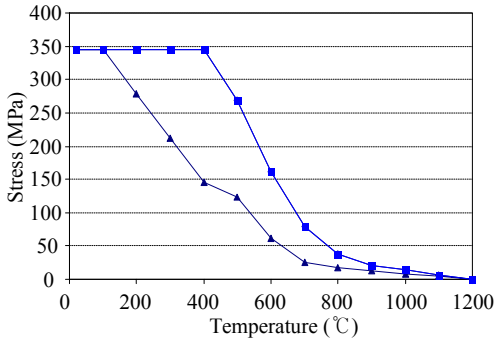

Figure 6. Proportional limit and effective yield strength versus temperature for the A992, Grade 50 steel (Fy = 345 MPa).

Figure 7 shows Poisson's ratio versus temperature relationship for the conventional steel. The plot is a regression line obtained from test data, and it is only valid up to 725°C. As shown in Figure 7, Poisson's ratio does not vary much up to 725°C, i.e., in the range between 0.287 and 0.317. Thus, the commonly used value of 0.3 was used in current studies, and it was assumed not to vary with temperature.

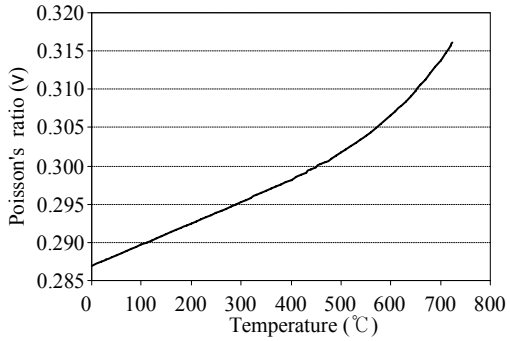

Figure 7. Poisson's ratio versus temperature for conventional steel (NIST NCSTAR 1-3D, 2005).

2.2 Properties of SFRM

Blaze Shield spray-applied fire resistive materials (SFRM) was used to model steel columns as a fire insulation for heat transfer analysis in current research, and its density is 240kg/m^3. Blaze Shield is a Portland cement based SFRM designed to provide fire resistance for structural steel and concrete in commercial construction.

According to NIST SP 1000-5(2004), the thermal conductivity and specific heat of Blaze Shield were determined as a function of temperature up to 1200°C and their test data were used in this research.

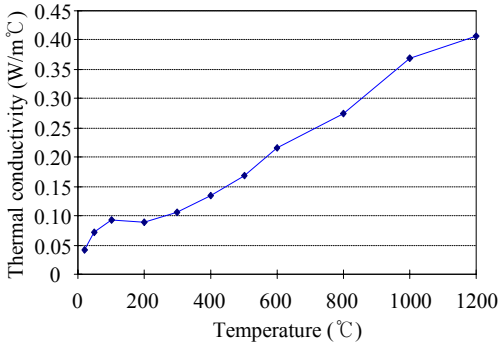

Figure 8. Thermal conductivity versus temperature for Blaze Shield II (SFRM) (NIST SP 1000-5, 2004).

The thermal conductivity was measured according to ASTM C 1113 test method for thermal conductivity of refractories by hot wire (Platinum Resistance Thermometer Technique) and it was used. Figure 8 shows the preliminary result for thermal conductivity as a function of temperature. The result shows a trend of increased thermal conductivity with increasing temperature. Also, Figure 9 shows specific heat versus temperature. As the case of the thermal conductivity, specific heat shows a trend of increased value with increasing temperature. Table 2 shows the properties of Blaze Shield (SFRM).

The strength and stiffness of the Blaze Shield (SFRM) is much less than those of the steel. Thus, the anticipated influence of the SFRM on the structural performance would be small. For this reason, the SFRM was omitted for all structural analysis.

The thicknesses of SFRM were yielded as Equation (7) by ICC-ES legacy reports, and they are 45mm for 3hour fire loading.

$$h = R / (1.01*(W/D)+0.66) \quad (7)$$

where, h = Thickness of fire-protection material ranging from 0.375 to 3.75 inches, R = Fire Resistance (hours), W = Weight of steel column (pounds per linear foot), and D = Heated perimeter of steel column (inches).

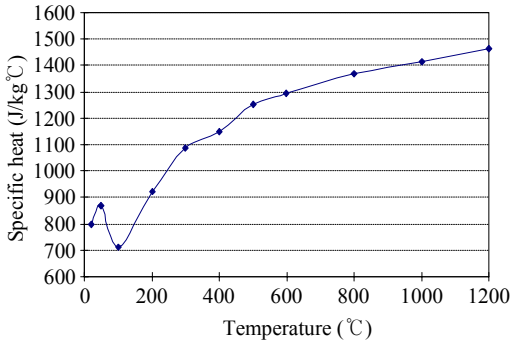

Figure 9. Specific heat versus temperature for Blaze Shield II (NIST SP 1000-5, 2005).

Table 2. Properties of Blaze-Shield (SFRM).

Temperature (°C)	Conductivity (W/m°k)	Specific Heat (J/kg°K)
20	0.042	797
50	0.072	868
100	0.093	712
200	0.088	924
300	0.106	1086
400	0.134	1149
500	0.169	1252
600	0.216	1293
800	0.275	1369
1000	0.369	1412
1200	0.407	1462

Note: Density = 240 (kg/m^3)

3. NUMERICAL MODEL

3.1 FEM Analysis Model

The analytical approach consists of two sequential analysis steps: (1) heat transfer analysis; and (2) structural analysis. The heat transfer analysis is conducted first to evaluate temperatures in the columns under the action of fire, and then the structural analysis is conducted to investigate the structural behavior due to temperature distributions obtained from the previous heat transfer analysis.

The heat transfer analysis is conducted to simulate the

transfer of heat from the fire to the structural members. The structural analysis is conducted to determine the complete structural response of the column subjected to the fire loading and axial load. The fire loading is first applied using the temperature-time history output obtained from previous heat transfer analysis.

Then, axial displacement is applied to the steel column to investigate the ultimate strength and the structural behavior of the steel column. In the structural analysis, nonlinear material properties and geometric nonlinearity are considered. Figure 10 shows an example of the FEM heat transfer model.

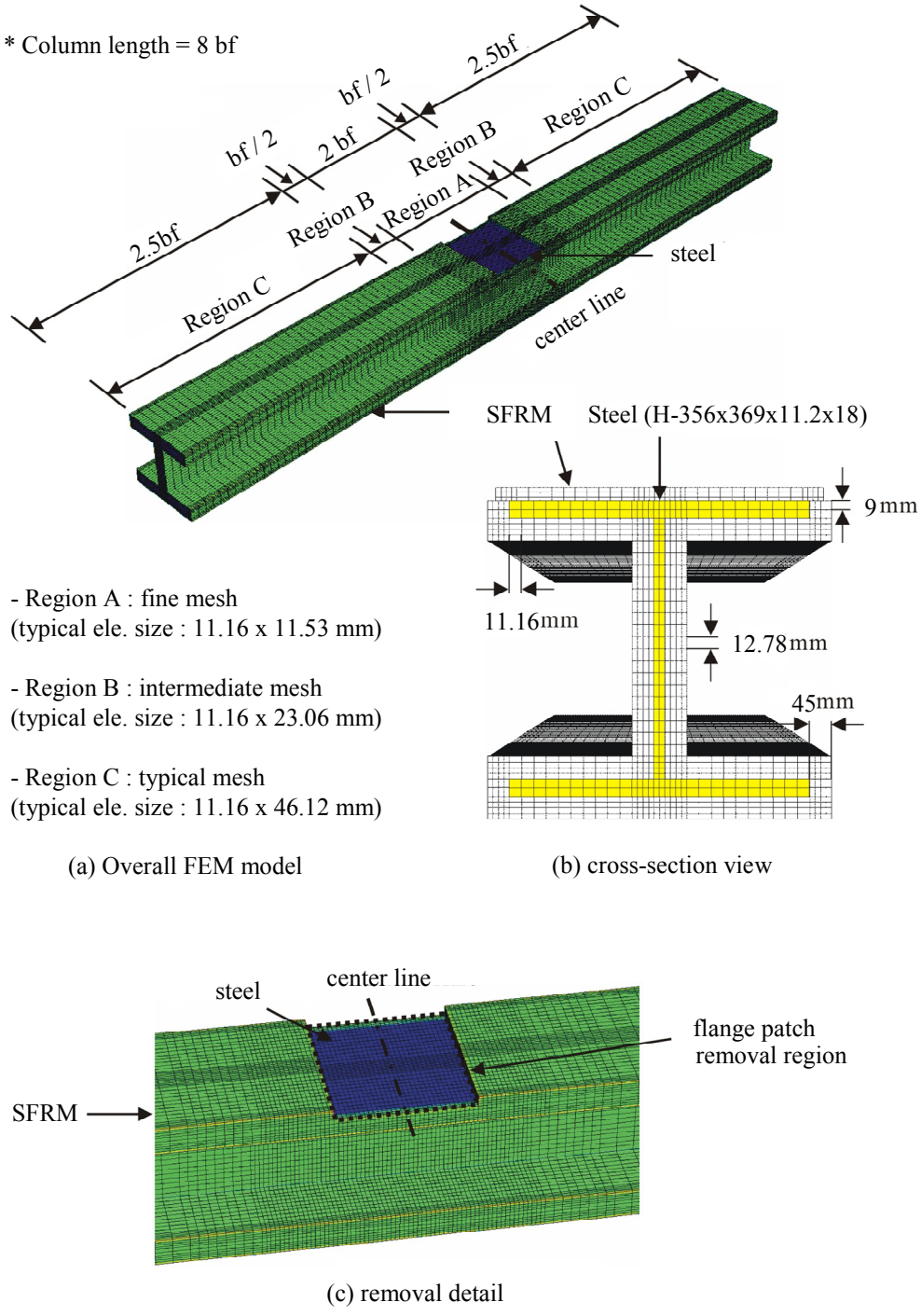

(a) Overall FEM model

(b) cross-section view

(c) removal detail

Figure 10. Example FEM heat transfer model.

The steel column, H-356x369x11.2x18 corresponding to W360x370x134 is encased by 45mm thick SFRM, and the SFRM is partially removed at the top flange of mid-height of column. Figure 10(a) shows the overall FEM model geometry and mesh. A cross-section view at mid-height of the column is shown in Figure 10(b). Figure 10(c) shows removal details of the SFRM.

As shown in Figure 10(a), the steel column is meshed in three different regions: Region A; B; and C. Region A has a very fine mesh, Region B has an intermediate mesh, and Region C has relatively a crude mesh as compared to Region A. A fine mesh was assigned where the SFRM is removed, and this is because a significant temperature gradient is expected within this region. DC3D8 element types were used to model both the steel and the SFRM. These are three-dimensional eight-node linear heat transfer elements, and include conduction heat transfer within steel and SFRM.

The finite element mesh used in each structural analysis is the same as the finite element mesh used in the corresponding heat transfer analysis. This simplified the assignment of temperature history results obtained from the heat transfer analyses as input to the structural analyses. SFRM was omitted from the FEM structural analysis models since the SFRM provides negligible resistance to axial compression relative to resistance provided by the column.

C3D8I elements were used to model the steel columns. These are three-dimensional eight-node continuum elements. All columns were modeled with a simple supported boundary condition. The effects of both residual stresses and out-of-plane were ignored in the model. This is because the current study focuses on the influence of the damaged SFRM on the axial load behavior of the columns in fire.

3.2 Analysis Parameters

In the current studies, both SFRM thinning removal (i.e., a reduction in SFRM thickness) and three specified fire durations of 60,120 and 180minutes were considered as analysis parameters.

Table 3 and Figure 11 summarize the analyses that were performed. The thinning removal cases treated a reduction in thickness of the SFRM on the flange. Five different SFRM thickness removal cases were analyzed, identified in Table 3. Shown in Table 3 are the dimensions of the patch removed, denoted as (wp) x (lp) x (tp) for the flange, where wp and lp are the width and length of the patch, and tp is the thickness of SFRM (0 tp: no removal, ¼ tp: ¼ removal).

The column treated in the analyses were H-356x369x11.2x18 (W360x370x134, G=134kg/m). They were made of Grade 50 steel (Fy=345Mpa), and the entire height of columns was 8bf (i.e., 2.952m). Each steel column was modeled with a simple supported boundary condition. The intended thickness of SFRM for these columns for a 3hour fire rating are 45mm. This column section and this thickness of SFRM are typical of steel building construction practices.

Table 3. Flange Thinning Removal Models.

Model name	Patch dimension (wp) x (lp) x (tp)	Removal in SFRM
FTRcut0	bf x 1/4 bf x 0 tp	No Removal
FTRcut1	bf x 1/4 bf x 1/4 tp	1 / 4 Removal
FTRcut2	bf x 1/4 bf x 1/2 tp	1 / 2 Removal
FTRcut3	bf x 1/4 bf x 3/4 tp	3 / 4 Removal
FTRcut4	bf x 1/4 bf x 4/4 tp	No SFRM

Note: wp = patch width, lp = patch length, tp = SFRM thickness, and bf = flange width

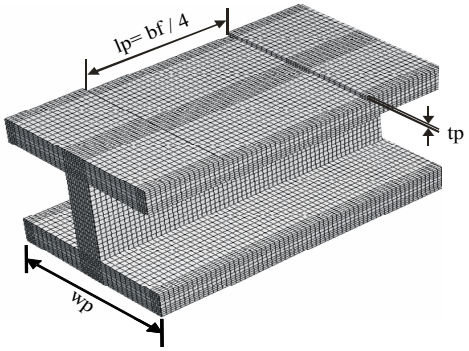

tp values : 0, tp / 4, tp / 2, 3tp / 4, and tp

Figure 11. FEM model detail.

3.3 FEM Heat Transfer Analysis

A transient heat transfer analysis was conducted. This is because temperatures in a member vary with time in fire, and an overall temperature history of the member needs to be solved for the following structural analysis. The time increment in each transient heat transfer analysis was controlled automatically by ABAQUS, and was done with the backward Euler method. The heat transfer analysis is nonlinear because the material properties are temperature-dependent. Also, radiation effects make the analysis nonlinear.

As a thermal loading for the heat transfer analysis, ASTM E119 standard fire curve was used. The temperature versus time curve of ASTM E119 is shown in Figure 12. ASTM E119 standard fire curve are guidelines for fire safe design of buildings and are not intended to represent the temperature-time history of an actual fire. For each FEM model, an initial temperature was specified as a room temperature, 20C.

Three basic heat transfer mechanisms described were considered in the FEM heat transfer model, and these are

conduction, convection and radiation. Nonlinear thermal material properties were also accounted for to predict correct temperature history. As described previously, required material properties in a heat transfer analysis are the thermal conductivity, density, and specific heat (Figure1, 2, 8, 9).

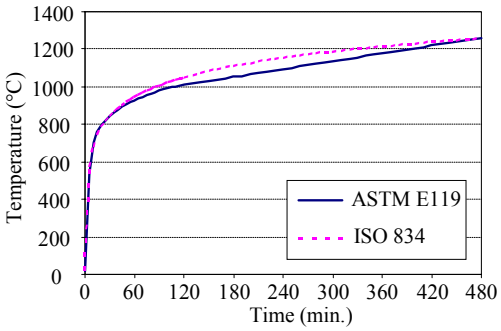

Figure 12. Temperature-time curves for ISO834 and ASTM E119 fires.

3.4 FEM Structural Analysis

Temperature results obtained from a corresponding previous transient heat transfer analysis were included in the structural analysis as an initial fire loading, and structural responses subjected to the axial loads resulting from the imposed axial displacement were investigated and studied.

All FEM structural analyses were conducted with displacement control of the steel column to obtain the maximum strength of the steel column and to capture post peak resistance behavior of steel columns after reaching the ultimate load. Fire loading was applied for specified fire durations of 60, 120, and 180minutes. Then, the distribution of steel temperatures was held constant, and column axial load was applied by controlling column axial displacement. Self-weight of steel columns was ignored in the analysis.

A nonlinear structural analysis was conducted. This nonlinear analysis includes large displacement effect, material nonlinearity, and geometrical nonlinearity. ABAQUS uses Newton's method to solve the nonlinear equilibrium equations. Thus, the solution is usually obtained as a series of time increments, with iterations to obtain equilibrium within each time increment.

4. RESULTS AND DISCUSSION

FEM analyses were performed for the flange thinning removal models (FTR models) in which the SFRM was reduced as a constant strip in thickness at the top flange of the column. The temperature results for all models obtained from the heat transfer analyses were included as an initial condition in the FEM structural analyses.

The curves of temperature versus fire duration for FTR models are plotted in Figure 13. The steel temperatures are plotted at four different selected locations (N1 through N4) along the flange and web of the cross section, and the selected cross section is at the mid height of the column where the SFRM is removed. Figure 13(b) shows the temperature versus fire duration curve of FTRcut1 model which has 1/4 removal of SFRM thickness. Temperatures at selected nodes increase almost similarly over the entire fire duration as the temperature curves of the perfectly insulated steel column. The maximum temperature in FTRcut1 model is at the top flange tip (N1), and is 704°C at fire duration of 3hours. The minimum temperature is at N3 location, and is 671°C. The temperature difference between the maximum and the minimum temperatures is only 33°C. This is because the SFRM remained at the top flange resists to fire loading. The temperature results of FTRcut2 (1/2 removal), FTRcut3 (3/4 removal) and FTRcut4 (No SFRM) models are presented in Figure 13(c) (d) (e). Similar results can be found in the rest of FTR series model. The steel temperatures increase as the removal size increases. In FTRcut4 model, the temperatures at the top flange (N1, N2, N3) increased significantly up to a fire duration of 30 minutes contrary to the temperature rise of other flange removal models. Thus, the complete removal of the SFRM leads to dramatic increases of steel temperature.

Figure 14 shows temperature versus fire duration curves by the thickness removal of SFRM. As shown in Figure14, the temperature for FTRcut3(3/4 removal) and FTRcut4(No SFRM) models at the top flange tip is 150°C, 490°C at a fire duration of 30 minutes, and the temperature difference is 340°C. Thus, the complete removal of the SFRM leads to dramatic rise of temperature and significantly reduces the fire resistance of steel column.

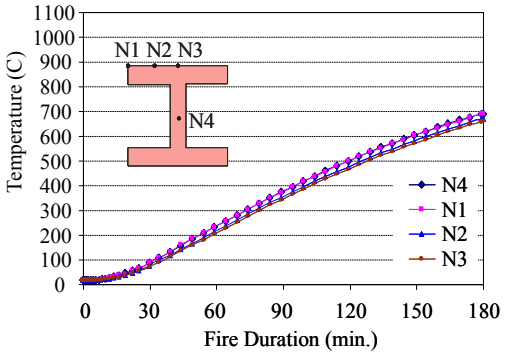

(a) No Removal

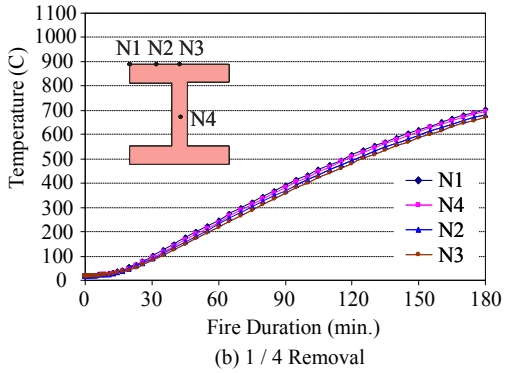

(b) 1 / 4 Removal

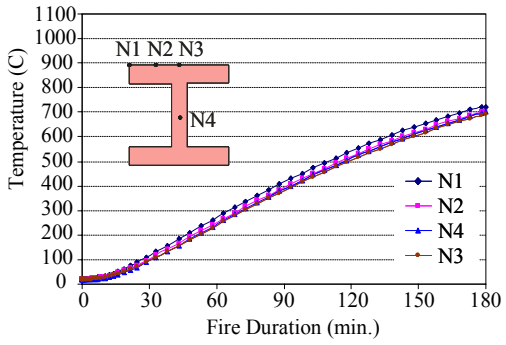

(c) 1 / 2 Removal

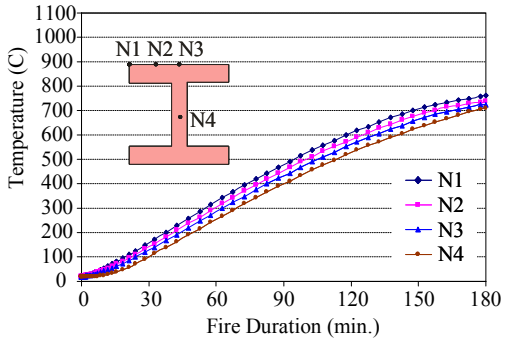

(d) 3 / 4 Removal

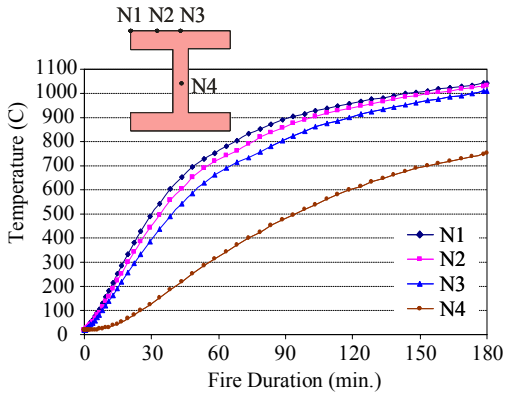

(e) No SFRM

Figure 13. Temperature versus fire duration curves at four different selected locations.

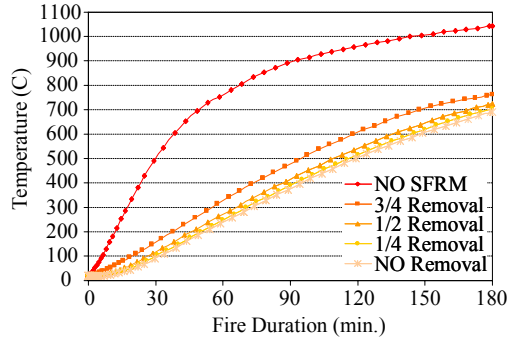

Figure 14. Temperature versus fire duration curves by the thickness removal of SFRM.

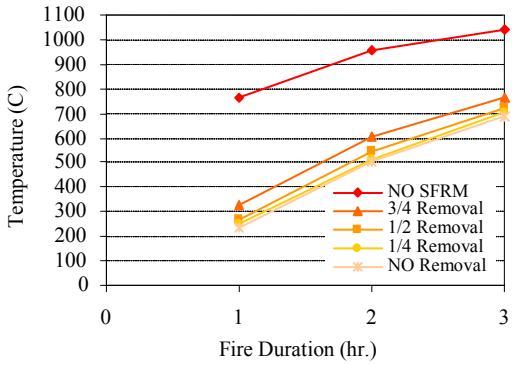

Figure 15. Maximum temperature versus fire duration relationship.

Figure 15 shows maximum temperature versus fire duration curves by the thickness of SFRM. In 3 hours fire duration with remnants of SFRM, temperatures of the column vary between 692°C(No removal) and 762°C(3/4 removal). Even though remnants of SFRM trivially remain, it can significantly decrease the temperature increases in columns in a fire. However, it is found that the complete removal of SFRM leads to the dramatic increases of steel temperatures. As shown in Figure, the temperature is 1042°C at a fire duration of 3hours. In that, the temperature difference between no removal model and complete removal model is almost 350°C. As stated above, even small remnants of SFRM tend to reduce significantly the temperature at any given fire duration.

Figure 16 shows P/Pu versus shortening curves for FTR models at fire durations of 60, 120 and 180minutes. Also, it shows P/Pu versus shortening curves according to the thickness of SFRM. As shown in Figures, the column axial load, P, is normalized by Pu which represents the column axial strength at room temperature. Also, included in the figures are axial load versus shortening relationships for the column perfectly insulated column in a fire, and bare steel column in a fire. As the removal size of the SFRM and fire duration increases, the capacity of the steel column decreases.

yielding occurs and the steel column fails with deformed shape shown in Figure 18.

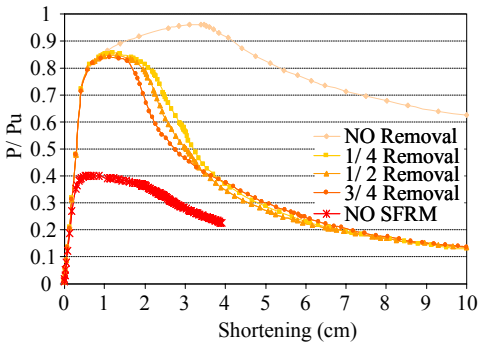

(a) 1 hour

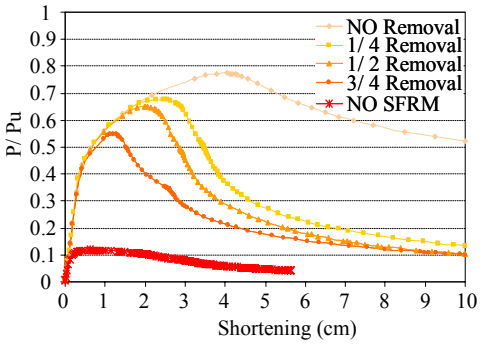

(b) 2 hours

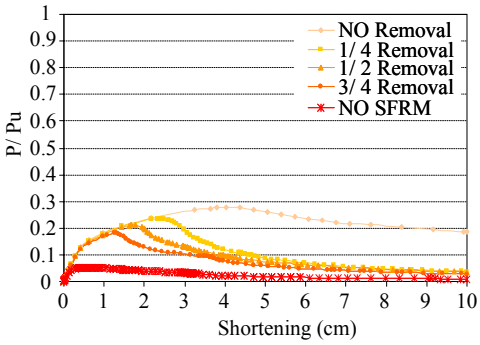

(c) 3 hours

Figure 16. P/Pu versus shortening curves at fire duration.

Figure 17 shows the capacity versus fire duration relationship for all models. The capacity is the maximum P/Pu. As shown in Figure17 and Table 4, the capacities of all models decrease as the fire duration increase. Also, as the flange thinning removal size increases the axial load capacity of the column decreases.

Figure 18 shows a deformed shape for FTRcut1 model. The deformed shape is for a normalized axial load, P/Pu of 0.255 with an axial shortening 5.33cm after the column was exposed to a fire duration of 120 minutes. As shown in Figure 18, the steel column failed at the mid height where the SFRM was reduced. This is due to material degradation caused by high steel temperatures. As shown in Figure 13(b), the temperatures at the top flange were 482°C-515°C at a fire duration of 120 minutes. According to Figure 4 of the steel stress-strain relationship at elevated temperature, the strength of the steel begins to reduce significantly at 500°C. Thus, the steel material yielding occurs and the steel column fails with deformed shape shown in Figure 18.

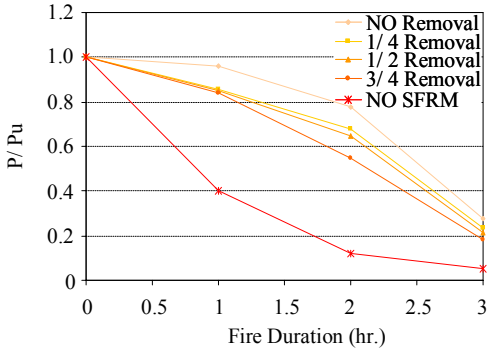

Figure 17. Capacity versus fire duration relationship.

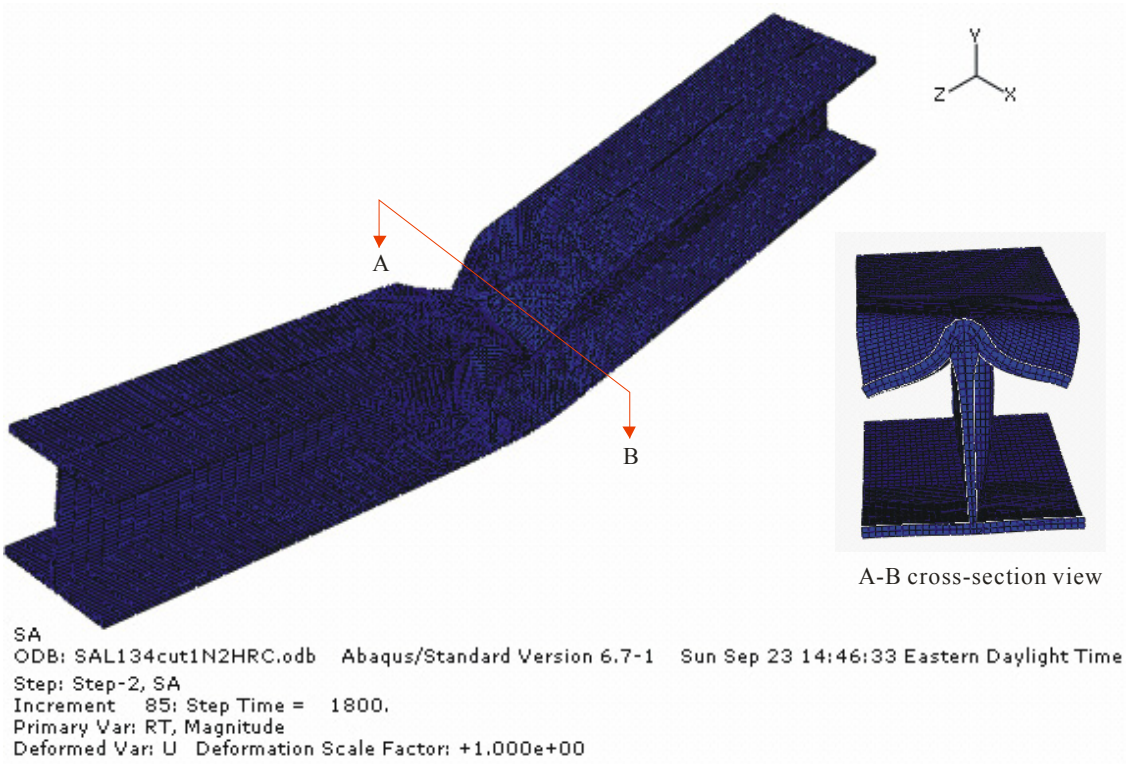

Figure 18. Deformed shape for FTRcut1 model at a fire duration of 2hours.

Table 4. Summary of axial load capacity for all models at various fire durations.

Fire Duration (min)	FTRcut0 (NoRemoval)	FTRcut1 (1/ 4 Removal)	FTRcut2 (1/ 2 Removal)	FTRcut3 (3/ 4 Removal)	FTRcut4 (No SFRM)
0	1.000	1.000	1.000	1.000	1.000
60	0.962	0.854	0.848	0.838	0.400
120	0.775	0.678	0.650	0.548	0.119
180	0.279	0.235	0.213	0.180	0.054

5. CONCLUSIONS

FEM analyses were performed for the flange thinning removal models (FTR models) in which the SFRM was reduced as a constant strip in thickness at the top flange of the column. From this study, the following conclusions can be drawn.

(1) The steel temperatures increase as the removal size increases. Also, the complete removal of the SFRM leads to dramatic rise of temperature and significantly reduces the fire resistance of steel column.

(2) The capacities of all models decrease as the fire duration increase. Also, as the removal size of the SFRM increases, the capacity of the steel column decreases.

(3) Even small remnants of SFRM led to an effective reduction of temperature at any given fire duration, and improved significantly the axial load capacity of a column as compared to the complete removal cases of SFRM.

6. FURTHER WORK

The current study focused on the influence of the damaged SFRM at the top flange, where considered only for strong axis of the column, regarding the axial load behavior of the columns in fire. However, it is also of an important interest that the fire behavior on the SFRM damaged at the web of the column (i.e., considering weak axis) is evaluated to investigate the governing failure patterns (e.g., by lateral-torsional buckling and/or by material yielding). Moreover, it may be expanded to the studies on fire performance of the steel columns protected partially by various fire resistive materials.

ACKNOWLEDGMENTS

The authors wish to thank the Kumoh National Institute of Technology for granting professor Kwak a sabbatical leave to undertake this research at the Lehigh University.

REFERENCES

ABAQUS Inc. (2007) ABAQUS Version 6.7-1 Documentation.

American Institute of Steel Construction, Inc. (AISC), “Steel Design Guide 19: Fire Resistance of Structural Steel Framing.” December, 2003, 123 pp.

American Society of Testing and Materials, ASTM E119: Standard Test Methods for Fire Tests of Building Construction and Materials, West Conshohocken, PA.

Blaze Shield II, SFRM Products, Isolatek International: Product information.

British Standards Institution (2001) Eurocode 3: Design of Steel Structures– Part 1.2: General Actions– Structural Fire Design, DD ENV 1993-1-2:2001, London.

Choi, S.K., Kim, S.B., Lee, C.N., Kim, S.S., Kim, H.Y., and Shin, H.J.(2005) "Numerical Study on the Fire Resistance Performance of the TSC Beam," Proceeding of Architectural Institute of Korea, 2005 Autumn, Vol.25, No.1, pp.551-554.

Franssen, J. M., Talamona, D., Kruppa, J., and Cajot, L. G. (1998) “Stability of Steel Columns in Case of Fire: Experimental Evaluation.” Journal of Structural Engineering, Vol. 124, No. 2, 158-163.

Huang, Z.F., and Tan, K.H. (2003) “Analytical Fire Resistance of Axially Restrained Steel Columns.” Journal of Structural Engineering, Vol. 129, No. 11, 1531-1537.

Hyeon, C., and Kim, M. H.(1990) "A Study on the Temperature Distribution of Thermally Protected Steel Column Exposed to the Fire," Proceeding of Architectural Institute of Korea, 1990 Autumn, Vol.10, No.2, pp.641-644.

International Code Council, Inc. (2002) “2003 International Building Code,”.

Janss, J. (1995) “Statistical Analysis for Fire Tests on Steel Beams and Columns to Eurocode 3: Part 1.2.” Journal of Constructional Steel Research, Vol. 33, No. 1-2.

Koo, B.Y. and Kang, M.M. (2004) "A Study on the Lateral-torsional Buckling of H-Beams at Elevated Temperature," Journal of Architectural Institute of Korea, Vol.20, No.2, pp.39-45.

Kohno, M., and Masuda, H., “Fire-Resistance of Large Steel Columns under Axial Load,” the CIB-CTBUH International Conference on Tall Buildings, Malaysia, May 2003.

Kwon, I.K., Jee, N.Y., and Lee, S.H.(2002) "Experimental Study on the Critical Temperature for Structural Elements such as Column and Beam Exposed to Fire Conditions," Journal of Architectural Institute of Korea, Vol.18, No.10, pp.45-52.

Kwon, K., Pessiki, S. and Lee, B. J. (2006) “An Analytical Study of the Fire Load Behavior of Steel Building Columns with Damaged Spray-Applied Fire Resistive Material,” ATLSS Report No. 06-25, Lehigh University.

Lamont, S., Usmani, A.S., and Drysdale, D.D. (2001) “Heat Transfer Analysis of the Composite Slab in the Cardington Frame Fire Tests,” Fire Safety Journal, Vol. 36, 815-839.

Lee, B. J., Pessiki, S. and Kohno, M. (2006) “Analytical Modeling of Large-Scale Fire Tests of Steel Box Columns with Damaged Fire Resistive Insulation,” ATLSS Report, Lehigh University.

Lie, T. T., and Stanzak, W.W. (1973) “Fire Resistance of Protected Steel Columns.” Engineering Journal, Vol. 10, No. 3, 82-94.

Min, J.K., Kang, S.W., Kim, M.H., and Kim, S.D.(2005) "Analytical Estimation on the Fire-Resisting Capacity of the iTECH Beam," Journal of Architectural Institute of Korea, Vol.21, No.78, pp.37-45.

National Fire Protection Association and Society of Fire Engineers (1988) SFPE Handbook of Fire Protection Engineering, First Edition.

Poh, K.W., and Bennetts, I.D. (1995) “Analysis of Structural Members under Elevated Temperature Conditions.” Journal of Structural Engineering, Vol. 121, No. 4, 664-675.

Poh, K.W., and Bennetts, I.D. (1995) “Behavior of Steel Columns at Elevated Temperature.” Journal of Structural Engineering, Vol. 121, No. 4, 676-684.

Ryder, N. L., Wolin, S.D., and Milke, J. A. (2002) “An Investigation of the Reduction in Fire Resistance of Steel Columns Caused by Loss of Spray-Applied Fire Protection,” Journal of Fire Protection Engineering, Vol. 12, 31-44.

Talamona, D., Franssen, J. M., Schleich, J. B., and Kruppa, J. (1997) “Stability of Steel Columns in Case of Fire: Numerical Modeling.” Journal of Structural Engineering, Vol. 123, No. 6, 713-720.

Tomecek, D.V., and Milke, J.A. (1993) “Study of the Effect of Partial Loss of Protection on the Fire Resistance of Steel Columns.” Fire Technology, Vol. 29, No. 1, 3-21.

Wong, M.B. and Ghojel, J.I. (2003) “Sensitivity Analysis of Heat Transfer Formulations for Insulated Structural Steel Components,” Journal of Fire Safety, Vol. 38,187-201.

(Data of Submission : 2008. 1.25)